

Structural and static magnetic properties of Ce-substituted NiZnCo ferrite nanopowders

TAI-XING HUANG, LE-ZHONG LI*, JUN YANG

Sichuan Province Key Laboratory of Information Materials and Devices Application, Chengdu University of Information Technology, Chengdu 610225, Sichuan, People's Republic of China

Ce-substituted NiZnCo ferrite nanopowders, $\text{Ni}_{0.5}\text{Zn}_{0.5}\text{Ce}_x\text{Co}_{0.1}\text{Fe}_{1.9-x}\text{O}_4$ ($0 \leq x \leq 0.20$), were synthesized by sol-gel auto-combustion method. The effect of Ce substitution on the structural and magnetic properties have been investigated. X-ray diffraction (XRD) and vibrating sample magnetometer (VSM) measurements were used to characterize structural and magnetic properties. XRD results indicate that the lattice parameter increases and the average crystallite size decreases with increasing Ce substitution. And CeO_2 secondary impurity phase formed with excess Ce substitution. The saturation magnetization and coercivity monotonically decrease with the increase of Ce substitution.

(Received July 2, 2015; accepted August 3, 2016)

Keywords: NiZnCo ferrite nanopowder, Sol-gel auto-combustion process, Ce substitution, Structure, Magnetic property

1. Introduction

The unique properties of ferrite nanopowders have generated more interest in the science community because high surface to volume ratio resulting in novel phenomena's of nanomagnetism such as superparamagnetism, magnetic quantum tunneling and spin-glasslike behavior etc. [1].

It is well known that the ferrites MFe_2O_4 with the spinel structure are based on a face-center cubic lattice of the oxygen ions. Each spinel unit cell contains eight formula units. In each unit cell, there are 64 tetrahedral sites (A sites) and 32 octahedral sites (B sites). Therefore, the chemical, structural, and magnetic properties of ferrite are strongly influenced by their composition and microstructure, which are sensitive to the preparation methodologies [2]. They show various magnetic properties depending on the cation distribution. Various cations can be placed in the structure of AB_2O_4 in A site and B site, which can result in the interesting physical and chemical properties in spinel ferrites [3].

Numerous workers have studied the effect of Ce^{3+} substitution in Bi ferrite [4, 5], Cu ferrite [6, 7], Co ferrite [8], Sr-Co ferrite [9], Co-Cr ferrite [10], Li ferrite [11] and NiCuZn ferrite [12]. In spinel ferrites, Q. Lin investigated the structural properties and cation distribution for Ce^{3+} doped NiCuZn ferrite [12]. To the best of our knowledge, no results have been reported about the effects of Ce^{3+} substitution on the structural and magnetic properties of NiZnCo spinel ferrite nanopowders.

In the present work, NiZnCo ferrite nanopowders

were prepared by sol-gel auto-combustion method which is a wet chemical synthesis method using nitrate, aim at low temperature synthesis and refine sample grain comparing to conventional ceramic method. Accordingly, in the present paper, we report our results on structural and magnetic properties of magnetic Ce^{3+} substituted NiZnCo ferrite nanopowders prepared by the sol-gel auto-combustion method.

2. Experimental procedures

The samples of $\text{Ni}_{0.5}\text{Zn}_{0.5}\text{Ce}_x\text{Co}_{0.1}\text{Fe}_{1.9-x}\text{O}_4$ ($x=0, 0.05, 0.10, 0.15, 0.20$) ferrite nanopowders were synthesized by sol-gel auto-combustion method. Stoichiometric quantities of analytical grade $\text{Zn}(\text{CH}_3\text{COO})_2 \cdot 2\text{H}_2\text{O}$, $\text{Ni}(\text{CH}_3\text{COO})_2 \cdot 4\text{H}_2\text{O}$, $\text{Fe}(\text{NO}_3)_3 \cdot 9\text{H}_2\text{O}$, $\text{Co}(\text{NO}_3)_2 \cdot 6\text{H}_2\text{O}$ and $\text{Ce}(\text{NO}_3)_3 \cdot 6\text{H}_2\text{O}$ were first dissolved in deionized water and stirred for 15 minutes. After the nitrates completely dissolved, the citric acid was added to the resulting solution and the molar ratio of citric acid and metal nitrates was taken as 1:1. Then, the prepared solution was continuously stirred for 3 hours at 80°C to form the gel precursors. To maintain the pH value at 7 an aqueous ammonia solution was added drop-wise after the gel precursors cooled to room temperature. The gel solution was dried at 85°C until a dry gel precursor was obtained. Finally, the dried gel was ignited in self-propagation combustion to obtain ferrite powders.

The phase identification of the prepared nanopowders was performed by DX 2700 X-ray diffractometer (XRD)

(Cu target, K_{α} radiation, 35 kV, 25 mA) at room temperature. The hysteresis loops of samples were measured at room temperature by using a TOEI VSM-5S-15 vibrating sample magnetometer (VSM).

3. Results and discussion

3.1. Structural properties

X-ray diffraction patterns of $Ni_{0.5}Zn_{0.5}Ce_xCo_{0.1}Fe_{1.9-x}O_4$ ferrite nanopowders are shown in Fig. 1. The different structural parameters of all samples are calculated according to XRD data and the results are shown in Fig. 2. The patterns match well with the characteristic reflections of cubic spinel structure. From it we can see that there is a CeO_2 secondary impurity phase when $x \geq 0.10$. This is mainly due to the fact that higher sintering temperature is needed to form crystallites for rare earth ions substitution ferrites. [12-14], which indicates that Ce^{3+} ions do not or partially form the solid solution with spinel ferrite by sol-gel auto-combustion method. In fact, the increase of lattice parameter in Fig. 2 conforms that Ce^{3+} ions have partially formed the solid co-solubility.

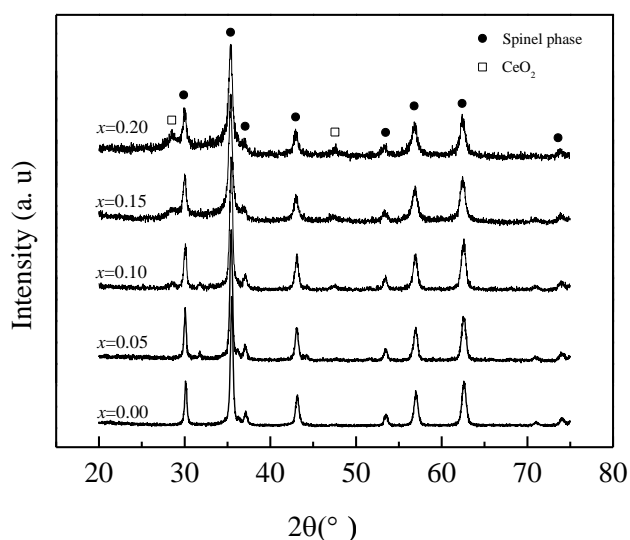


Fig. 1. X-ray diffraction patterns of $Ni_{0.5}Zn_{0.5}Ce_xCo_{0.1}Fe_{1.9-x}O_4$ ferrite nanopowders.

The lattice parameter (a) of the samples is calculated using the relation [15]:

$$a = d_{hkl} \sqrt{h^2 + k^2 + l^2} \quad (1)$$

where $(h \ k \ l)$ are the Miller indices and d_{hkl} is the inter-planar spacing. The average particle size is calculated according to Debye-Scherrer equation [15-17]:

$$D = \frac{0.9\lambda}{\beta \cos \theta} \quad (2)$$

From Fig. 2 it is clear that, the lattice parameter (a) increases and the average crystallite size calculated by Debye-Scherrer's equation decreases with the increase of Ce substitution. The increase of lattice parameter is attributed to the ion replacement of Fe^{3+} ion with smaller radii (0.64 Å) by Ce^{3+} ion with larger radii (1.03 Å) and Ce^{3+} ion partially enters into lattice which are confirmed by reference 12. The variations of lattice parameter will lead to the lattice strains which can introduce the inter stress, and the inter stress will hinder the growth of grains [18-20]. Furthermore, the excessive Ce substitution results in the Ce^{3+} ion separating out from the spinel structure and forming CeO_2 phase will diffuse to the crystallite boundaries and hinder the crystallite growth. Therefore, the average crystallite size decreases with the increase of Ce substitution.

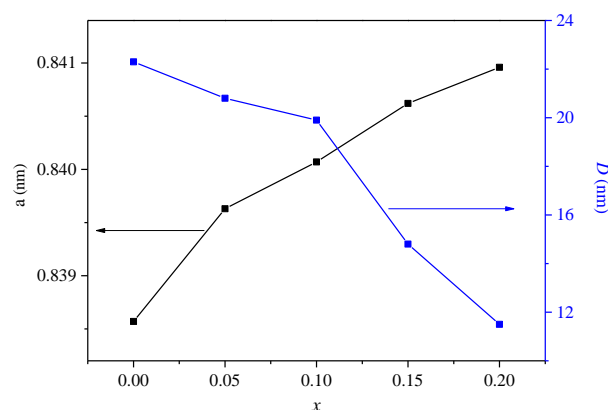


Fig. 2. Lattice parameter (a) and average crystallite size (D) of $Ni_{0.5}Zn_{0.5}Ce_xCo_{0.1}Fe_{1.9-x}O_4$ ferrite nanopowders.

3.2. Magnetic properties

Fig. 3 shows the hysteresis loops of $Ni_{0.5}Zn_{0.5}Ce_xCo_{0.1}Fe_{1.9-x}O_4$ ferrite nanopowders. It is observed that the hysteresis loops of NiZnCo ferrite nanopowders without and with Ce substitution are that of typical ferrimagnet. Furthermore, the saturation magnetization (M_s) and coercivity (H_c) of nanopowders as a function of Ce substitution (x) are shown in Fig. 4. The saturation magnetization (M_s) and the coercivity (H_c) monotonically decrease with the increase of Ce substitution.

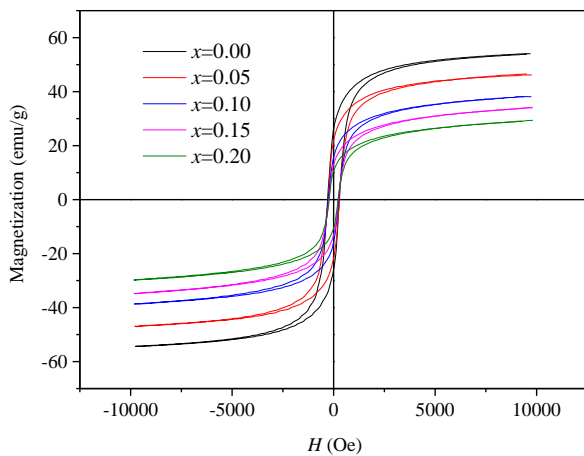
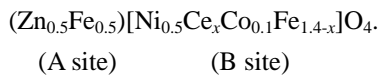


Fig. 3. Hysteresis loops of $Ni_{0.5}Zn_{0.5}Ce_xCo_{0.1}Fe_{1.9-x}O_4$ ferrite nanopowders.

Magnetic properties of ferrites are sensitively dependent on the structure, composition, defects, crystallite size, internal strain and cation distribution. According to Néel's two sublattice model of ferrimagnetisms [21] and Ce^{3+} ion enters octahedral sites [10, 12], the cations distribution can be written as follows:



And the magnetic moment in Bohr magneton of $Ni_{0.5}Zn_{0.5}Ce_xCo_{0.1}Fe_{1.9-x}O_4$ ferrite nanopowders is calculated by the following equation:

$$M = |M_B - M_A| = |5.8 - 2.46x| \quad (3)$$

Where M_A and M_B are the magnetic moments in the A and B sites, and the magnetic moments of Zn^{2+} , Ni^{2+} , Ce^{3+} , Co^{2+} , and Fe^{3+} ions are 0, 2, 2.54, 3, and $5 \mu_B$, respectively. Simultaneously, the term of saturation magnetization (M_s) is defined as the vector sum of magnetic moment per unit cell, and is written as the following equation:

$$M_s = \frac{8M}{a^3} \quad (4)$$

Thus, according to equations (3) and (4), and the increase of lattices parameters (a) with Ce substitution, M_s monotonically decreases with the increase of Ce substitution.

In addition, the variations of lattice parameter will lead to the lattice strains which can introduce the inter stress, and the inter stress will also result in the decrease of M_s . Furthermore, the formation of CeO_2 impurity phase is another reason of decreasing M_s .

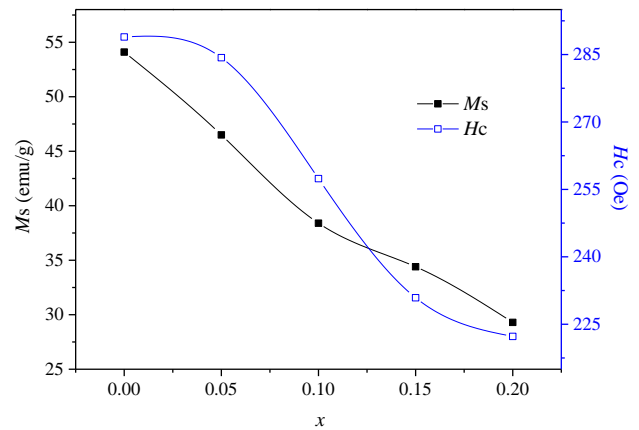


Fig. 4. M_s and H_c of $Ni_{0.5}Zn_{0.5}Ce_xCo_{0.1}Fe_{1.9-x}O_4$ ferrite nanopowders.

The coercivity (H_c) of ferrite nanopowders as a function of Ce substitution (x) is shown in Fig. 4, which indicates that H_c monotonically decreases with the increase of Ce substitution. The decrease in the H_c values is mainly due to the decrease in magnetocrystalline anisotropy which causes by the substitution of weaker magnetic moment ion. In addition, according to Stoner-Wohlfarth single domain theory [22], H_c decreased with the decrease of grain size when the grain is single domain structure. In present work, H_c and average crystallite size decrease with the increase of Ce substitution. Thus, another possible reason of H_c decrease is the single domain structure of grain.

4. Conclusions

Ce-substituted NiZnCo ferrite nanopowders, $Ni_{0.5}Zn_{0.5}Ce_xCo_{0.1}Fe_{1.9-x}O_4$ ($0 \leq x \leq 0.20$), have been synthesized by sol-gel auto-combustion method. The structural and static magnetic properties of nanopowders have been investigated and the following results have been obtained:

(1) The XRD results indicate that the lattice parameter increases and the average crystallite size decreases with the increase of Ce substitution. Furthermore, there is a CeO_2 secondary impurity phase when $x \geq 0.10$.

(2) The hysteresis curves of the nanopowders exhibit that the saturation magnetization and the coercivity monotonically decrease with the increase of Ce substitution.

Acknowledgments

This work is financially supported by the Research Fund for Young Academic Leaders of CUIT under Grant no. J201306.

References

- [1] M. S. Khandekar, R. C. Kambale, J. Y. Patil, Y. D. Kolekar, S. S. Suryavanshi, *J. Alloys Compd.* **509**, 1861 (2011).
- [2] F. Li, J. J. Liu, D. G. Evans, X. Duan, *Chem. Mater.* **16**, 1597 (2004).
- [3] S. T. Alone, S. E. Shirsath, R. H. Kadam, K. M. Jadhav, *J. Alloys Compd.* **509**, 5055 (2011).
- [4] S. Gupta, M. Tomar, V. Gupta, *J. Magn. Magn. Mater.* **378**, 333 (2015).
- [5] M. Arora, M. Kumar, *Ceram. Int.* **41**, 5705 (2015).
- [6] M. S. Khandekar, N. L. Tarwal, J. Y. Patil, F. I. Shaikh, I. S. Mulla, S. S. Suryavanshi, *Ceram. Int.* **39**, 5901 (2013).
- [7] M. A. Malana, R. B. Qureshi, M. N. Ashiq, Z. I. Zafar, *Mater. Res. Bull.* **48**, 4775 (2013).
- [8] G. Bulai, L. Diamandescu, I. Dumitru, S. Gurlui, M. Feder, O. F. Caltun, *J. Magn. Magn. Mater.* **390**, 123 (2015).
- [9] H. Choi, A. Fuller, J. Davis, C. Wielgus, U. S. Ozkan, *Appl. Catal. B: Environ.* **127**, 336 (2012).
- [10] G. Mustafa, M. U. Islam, W. Zhang, Y. Jamil, M. A. Iqbal, M. Hussain, M. Ahmad, *J. Magn. Magn. Mater.* **378**, 409 (2015).
- [11] V. Verma, R. K. Kotnala, V. Pandey, P. C. Kothari, L. Radhapiyari, B. S. Matheru, *J. Alloys Compd.* **466**, 404 (2008).
- [12] Q. Lin, C. Lei, Y. He, J. Xu, R. Wang, *J. Nanosci. Nanotechnol.* **15**, 2997 (2015).
- [13] G. Dixit, J. Pal Singh, R. C. Srivastava, H. M. Agrawal, *J. Magn. Magn. Mater.* **324**, 479 (2012).
- [14] C. Sun, K. Sun, *Solid State Commun.* **141**, 258 (2007).
- [15] B. D. Cullity, *Elements of X-ray Diffraction*, Addison Wesley Publishing: Massachusetts, 1959.
- [16] M. H. Mahmoud, C. M. Williams, J. Cai, I. Siu, J. C. Walker, *J. Magn. Magn. Mater.* **261**, 314 (2003).
- [17] M. H. Ibrahim, M. S. Seehra, G. Srinivasan, *J. App. Phys.* **75**, 6822 (1994).
- [18] J. C. Debnath, R. Zeng, D. P. Chen, S. X. Dou, *Mater. Sci. Eng. B* **177**, 48 (2012).
- [19] D. Li, Y. D. Huang, N. Sharma, Z. X. Chen, D. Z. Jia, Z. P. Guo, *Phys. Chem. Chem. Phys.* **14**, 3634 (2012).
- [20] F. Hong, Z. X. Cheng, X. L. Wang, *J. Appl. Phys.* **112**, 013920 (2012).
- [21] D. F. Wan, X. L. Ma, *The Physics of Magnetism*, UESTC Press: Chengdu, 1994.
- [22] E. C. Stoner, E. P. Wohlfarth, *IEEE Trans. Magn.* **27**, 3475 (1991).

*Corresponding author: lezhongli@cuit.edu.cn